Desalination 342 (2014) 43–51

Contents lists available at ScienceDirect

Desalination

journal homepage: www.elsevier.com/locate/desal

Electrodeionization of low-concentrated multicomponent Ni^{2+}-containing solutions using organic–inorganic ion-exchanger

Yu.S. Dzyazko *, L.N. Ponomaryova, L.M. Rozhdestvenskaya, S.L. Vasilyuk, V.N. Belyakov

V.I. Vernadskii Institute of General & Inorganic Chemistry of the NAS of Ukraine, Palladin Ave. 32/34, 03142 Kiev 142, Ukraine

HIGHLIGHTS

- Composite ion exchanger was obtained by modification of flexible cation-exchange resins with zirconium phosphate.
- This material was applied to electrodeionization processes.
- The method of Ni^{2+} removal from combining solutions, which contain also Ca^{2+} and Mg^{2+}, has been developed.

GRAPHICAL ABSTRACT

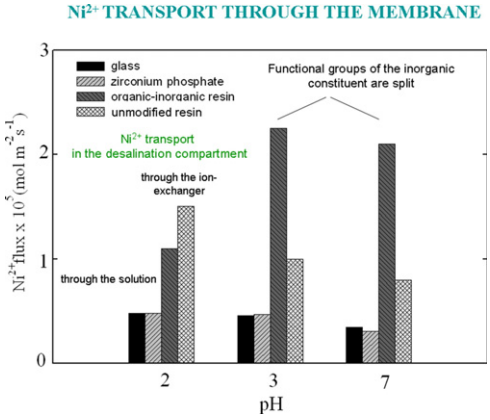

ARTICLE INFO

Article history:
Received 9 July 2013
Received in revised form 2 November 2013
Accepted 7 November 2013
Available online 19 December 2013

Keywords:
Ion-exchange membrane
Ion-exchange resin
Electrodialysis
Electrodeionization
Organic–inorganic ion-exchanger and membrane
Zirconium hydrophosphate
Nanoparticles
Aggregates

ABSTRACT

Organic–inorganic ion-exchangers have been obtained by modification of gel-like flexible resin with zirconium hydrophosphate, which form both single and aggregated nanoparticles in the polymer matrix. Insertion of the inorganic constituent into the resin up to 40 mass % was found to increase electrical conductivity of the resin from 0.2 to 0.7 Ω^{-1} m^{-1}. Total ion-exchange capacity also increases from 600 to 1800 mol m^{-3}. The organic–inorganic ion-exchanger with the highest amount of the inorganic constituent was used for electrodeionization processes to remove Ni^{2+} from low-concentrated solutions containing also hardness ions and organic substances. The "once-through" processes have been developed based on ion transport investigation under variation of the initial pH, concentration, and flow velocity of the solution being purified. Residual Ni^{2+} content in the solution was 0.7–0.9 ppm, the energy consumptions have been estimated 0.4–0.7 kWh per 1 m^3. The organic–inorganic ion-exchanger was found to demonstrate stability against fouling with organic substances as opposed to the unmodified resin.

1. Introduction

Electrodeionization (EDI) is a technique combining ion exchange and electrodialysis [1]. The potential gradient causes transport of species through the ion-exchanger bed and membranes, and the ion-exchanger is regenerated continuously by this manner. Thus EDI

* Corresponding author. Tel.: +380 444240462; fax: +380 444243070.
E-mail addresses: dzyazko@ionc.kiev.ua, dzyazko@hotmail.com (Y.S. Dzyazko).

0011-9164/$ – see front matter © 2013 Elsevier B.V. All rights reserved.
http://dx.doi.org/10.1016/j.desal.2013.11.030

permits the removal of species from a solution on the one hand and their concentration in the liquid phase on the other hand. Now EDI processes are applied mainly to demineralization of brackish water and its purification from organic matters traces. Water of geothermal searches [2,3], groundwater [4] and tap water [5] can be treated by means of this technique, which allows us to obtain drinking [6–8] or ultrapure water [9] as well as water for boilers [10] and power plants [11]. EDI method was also applied to the purification of phosphoric acid [12] and caprolactam [13].

EDI processes are highly developed for the removal of alkaline cations and some anions: Cl^-, SO_4^{2-} etc. The attempt to use this method for the recovery of bacteria and endotoxins from aqueous media is also known [14]. However, electrodeionization of the solutions, which contain hardness or d-metal ions, is usually complicated with formation of insoluble compounds on cation-exchange membranes and ion-exchanger particles [15,16]. The first way to solve this problem is to use a flexible cation-exchange resin, which contains 2% divinylbenzene (DVB) [16–22]. Another way is determination of optimal operation conditions. For instance, regular change of polarity has been developed to prevent the deposition of Ca and Mg compounds [23]. Previous acidification of the initial solution was proposed [19], cyclic operation of the solution passage through the ion-exchanger bed was also suggested for Ni^{2+} [19,24] and Cu^{2+} [24] removal. The process with bipolar membrane has been investigated for Ni^{2+} recovery [25].

In the case of electrodeionization of multicomponent solutions, which contain d-metal ions as well as Ca^{2+} and Mg^{2+}, hardness ions are removed preferably [19,20]. Moreover, resins are gradually poisoned with organic substances [26]. The use of zirconium hydrophosphate (ZHP) hydrogel allows us to increase Ni^{2+} removal degree [27], since the inorganic ion-exchangers of this type are selective towards d-metal ions [20,28]. The selectivity is explained by complex formation of sorbed ions with phosphorus-containing groups [28,29]. However, mechanical strength and chemical stability of hydrogel-like ion-exchangers is lower in a comparison with polymer materials.

The use of organic–inorganic ion-exchangers obtained by modification of polymer with inorganic nanoparticles can be a solution of the problems. These materials are selective towards toxic ions [30–34] and stable against fouling with organic substances [26]. Thus, the aim of the work was to investigate the EDI processes, which involve organic–inorganic ion-exchangers, in order to remove d-metal species from solutions containing also hardness ions and organics like humates. Moreover, we intended to determine the optimal operation conditions, at which the removal of toxic ionic impurities is the most complete.

Nickel ions were chosen as model species due to the practical importance of their recovery from waste solutions. Salts of this metal are widely used for electroplating to manufacture coatings with high corrosion and temperature resistance [35]. The extensive utilization of Ni-containing products leads to environmental pollution, this causes pathological effects in humans varying from contact dermatitis to lung fibrosis, cardiovascular and kidney diseases, and even cancer. Owing to this, nickel content in wastes is strongly controlled.

2. Experimental

2.1. Ion-exchangers

Dowex 50WX-2 resin (Dow Chemical) has been chosen as a model polymer matrix. This gel-like cation-exchanger containing 2% DVB was used successfully for the removal of divalent ions from aqueous solutions [16–22].

The ion-exchanger was modified according to the method, which had been developed for resins containing 8% DVB [26,34,36]. A weighted amount of the resin was impregnated with a 1 M $ZrOCl_2$ solution for 24 h, then treated with a 1 M H_3PO_4 solution, washed with deionized water, and dried in a desiccator over $CaCl_2$ at room temperature down to constant mass. The dry sample was treated in deionized water with ultrasound at 3×10^5 Hz using a Bandelin cleaning device (Bandelin). The treatment was necessary to remove ZHP from outer particle surface. The cleaning completeness was controlled with a JEOL JSM 6700F scanning electron microscope (Jeol). Previously a layer of platinum was deposited onto the particle surface at 3 Pa using a JEOL JFC-1600 Auto fine coater (Jeol).

The synthesis procedure was repeated several times; after each modification cycle a sample was taken for further investigations.

Individual ZHP was obtained by direct deposition from $ZrOCl_2$ with H_3PO_4 solution followed by dispergation in octane-filled column [37]. Hydrogel particles were dried in air down to constant mass, ZHP xerogel formed by this manner.

2.2. Characterization of the ion-exchangers

The total ion-exchange capacity (towards Na^+, $\bar{A}_{Na}$) of the samples was determined by treatment of their H-forms with a 0.1 M NaOH solution. Then the samples were washed up to neutral reaction of the effluent and regenerated with a 3 M H_2SO_4 solution, which was analyzed using a PFM-U4.2 flame photometer (Analitpribor).

The dependence of ion-exchange capacity of the samples towards Na^+ ions on pH was determined as follows. A 0.1 M NaCl solution, which had been previously acidified with HCl down to predetermined pH, was passed through an ion-exchange column similarly to [37]. The passage was stopped, when the solution conductivity at the inlet and outlet became approximately equal. A HI 9932 conductometer (Hanna Instruments) was used for the measurements. After loading, the samples were washed with water, dried at room temperature and treated with a 3 M H_2SO_4 solution. The effluent was analyzed as mentioned above.

Swelling was investigated by means of volumetric measurements before and after contact of air-dry samples with water [38].

TEM images were obtained using a JEOL JEM 1230 transmission electron microscope (Jeol), SEM method was also applied as described in Section 2.1, particularly for elemental analysis. The samples were previously crushed and treated with ultrasound.

Electrical conductivity of H-forms of the ion-exchangers was measured at 298 K similarly to [26,34,39]. The sample was washed with deionized water to remove additionally sorbed electrolyte, placed into a prismatic cell between platinum electrodes, then deionized water was added as a non-conductive medium. The measurements were carried out using an Autolab impedance system at 10^{-2}–10^6 Hz and 298 K. The ion-exchanger conductivity was determined from frequency spectra of the real part of admittance.

2.3. Ion exchange under dynamic conditions

Tap water, which contained ≈0.9 mol m^{-3} Ca^{2+}, 0.3 mol m^{-3} Mg^{2+} as well as 2.5–2.8 ppm TOC (total organic carbon), and $NiSO_4 \cdot 7H_2O$ salt were used for preparation of multicomponent solution (0.3 mol m^{-3} Ni^{2+}). The solution was passed through the column (0.8 cm of a diameter) with a flow velocity of 0.54 dm^3 h^{-1}. The volume of ion-exchanger in the column was 5 cm^3. The solution at the column outlet was analyzed with atomic absorption method using a Pye Unicam 8800 UV/VIS device (Philips) at the wavelength of 232 nm. The removal degree (*RD*) of ions was estimated as:

$$RD = \frac{C - C'}{C} \times 100\% \quad (1)$$

Here *C* and *C ′* are the concentration of species at the inlet and outlet respectively.

2.4. Experimental set-up for electrodeionization

The experimental set-up, which involved a three-compartment cell, three separate liquid lines, power supplier and measurement instrumentation, was similar to that described earlier [20,40,41]. Two cells with different geometric parameters were used. The effective area of the membranes and electrodes was 10 cm^2 (1 cm × 10 cm) and 100 cm^2 (10 cm × 10 cm) for the home-made (1) and produced by Electrocell (2) cells respectively. The distances between two membranes and bed height were 1 cm and 10 cm respectively for each cell. Electrodes made of platinized titanium were used.

2.5. Investigation of EDI processes

H_2SO_4 and HCl solutions (250 cm^3 of each) were circulated through the anode and cathode compartments respectively; their initial concentration was 1 M. Hydrochloric acid was needed to prevent $CaSO_4$ deposition in the cathode compartment.

Tap water, the composition of which was similar to that described in Section 2.3, was used for preparation of Ni^{2+}-containing solutions. The solution thermostated at 298 K was passed through the center compartment of the cell according to "once-through" operation from bottom to the top. The cell voltage (U) was kept at 5 V. The catholyte as well as the solution at the outlet of the center compartment were analyzed with atomic absorption method as mentioned above. The electrical conductivity and pH of the solution passing through the ion-exchanger bed were also measured.

2.5.1. Effect of initial pH of Ni^{2+}-containing solution

The cell 1, in which the electrode compartments were separated from the center chamber with homogeneous Nafion 117 cation-exchange membranes (DuPont), was used. The center compartment was filled with unmodified or organic–inorganic (eight modified with ZHP) ion-exchange resins. The processes, which involved ZHP and inert glass particles, were also studied. Unmodified resin contained initially ≈100 mol m^{-3} Ni^{2+} in order to avoid a decrease of the bed height due to $Ni^{2+} \rightarrow H^+$ exchange. Since no decrease of volume of the modified resin and ZHP occurs, H-forms of these materials were used.

The solution containing 0.3 mol m^{-3} Ni^{2+} was acidified previously with H_2SO_4 down to pH 3 or 2, or remained without acidification. It was passed through the center compartment with a flow velocity of 3.6 dm^3 h^{-1}. The EDI processes were carried out for 20 h.

TOC content in the resins was determined by means of Pregl combustion method [42] after the end of the process. The amount of carbon, which is a constituent of organic matters sorbed by ion-exchangers, was estimated as a difference between TOC amounts in the resins before and after the EDI process.

2.5.2. Effect of flow velocity of the solution being purified

Flow velocity of a Ni-containing solution was varied in the series of experiments, which involved eight modified resins. The solution was previously acidified down to pH 3. Other experimental conditions were similar to those described in Section 2.5.1. After the process was finished, the ion-exchanger was removed from the cell, mixed, washed and regenerated as mentioned in Section 2.1. Ni^{2+} content in the effluent was determined.

2.5.3. Effect of initial concentration of Ni^{2+}-containing solution

Initial Ni^{2+} content in the solution, which had been acidified previously down to pH 3, was varied. The solution was passed through the center compartment with a flow velocity of 1.2 dm^3 h^{-1}. Eight modified ion-exchange resins were used. Other experimental conditions were similar to those described in Section 2.5.1.

2.5.4. Long-time electrodeionization

Cell 2 was used for long-time electrodeionization of Ni^{2+}-containing solution. The cathode and anode compartments were separated from the center chamber with cation-exchange Nafion 117 and anion-exchange AMI-7001 (Membrane International) membranes. No previous acidification of the solution was performed. The first experiment provided the solution passage through the ion-exchanger bed with a flow velocity of 3 dm^3 h^{-1}, the solution contained initially 0.3 mol m^{-3} Ni^{2+}. Other experiment was performed at initial Ni^{2+} concentration of 0.15 mol m^{-3} and flow velocity of 12 dm^3 h^{-1}. The processes have been carried out at 5 V for 70 h.

3. Results and discussion

3.1. Characteristics of the ion-exchanger

Modification of the resin with inorganic constituent causes considerable increase in ZHP content (up to 40.1 mass %, Table 1). The samples with higher content of the inorganic constituent demonstrate low mechanical strength and were not investigated.

As seen from Fig. 1, the modified ion-exchanger contains both non-aggregated nanoparticles (7–14 nm) and their aggregates (from 30 to 50 nm up to several microns). In opposite to [30–33], where modified macroporous resins were considered, single nanoparticles have been obtained in the gel-like flexible resin. As known, swollen polymer ion-exchange materials consist of gel-like fields, where nanosized clusters and channels are located [43,44]. Clusters and channels, which contain functional groups, are responsible for ion transport. Thus non-aggregated nanoparticles can be placed there.

Small aggregates can occupy voids between gel-like fields, the micron particles are evidently located in structure defects, which exist even in dry polymer. The defects are seen in Fig. 1c as chelate-like formations, large ZHP aggregates are also visible.

The ion-exchangers demonstrate sufficient increase of ZHP content up to the fifth modification cycle (Table 1). No considerable growth of amount of the inorganic constituent has been found after further modification. A molar ratio of Ph:Zr in ZHP particles slightly decreases for twice modified sample in a comparison with once modified resin. This indicates lower phosphorus content in the inorganic constituent, which is formed during the second modification cycle. ZHP incorporated into the polymer matrix is characterized by higher molar ratio of Ph:Zr, than individual inorganic ion-exchanger. This is probably due to particle formation in nano- and microreactors (clusters, voids between gel fields, and structure defects).

The highest swelling has been found for the once modified sample, further modification causes deterioration of swelling. Perhaps this is a result of the influence of the inorganic particles on the labile polymer. Regarding the non-modified resin, hydration shell of counter-ions (H^+) can be unfinished due to small distance between functional groups [45]. Stretching of the polymer causes an increase of this distance and complete formation of the hydration shell. Moreover, location

Table 1
Characteristics of ion-exchangers.

Number of modification cycle	ZHP mass content, %	Molar ratio of Ph:Zr	$\bar{A}_{Na}$, mol m^{-3}	Swelling, %	Electrical conductivity, Ω^{-1} m^{-1}
0	–	–	569	75	0.20
1	20.9	1.60:1	462	120	0.21
2	25.0	1.4:1	612	110	0.27
3	29.8	1.4:1	1064	100	0.28
4	33.5	1.4:1	1406	90	0.33
5	38.2	1.4:1	1711	85	0.38
6	38.7	1.4:1	1775	75	0.42
7	39.5	1.4:1	1778	65	0.46
8	40.1	1.4:1	1791	60	0.70
ZHP	100	0.7	2000	–	0.05

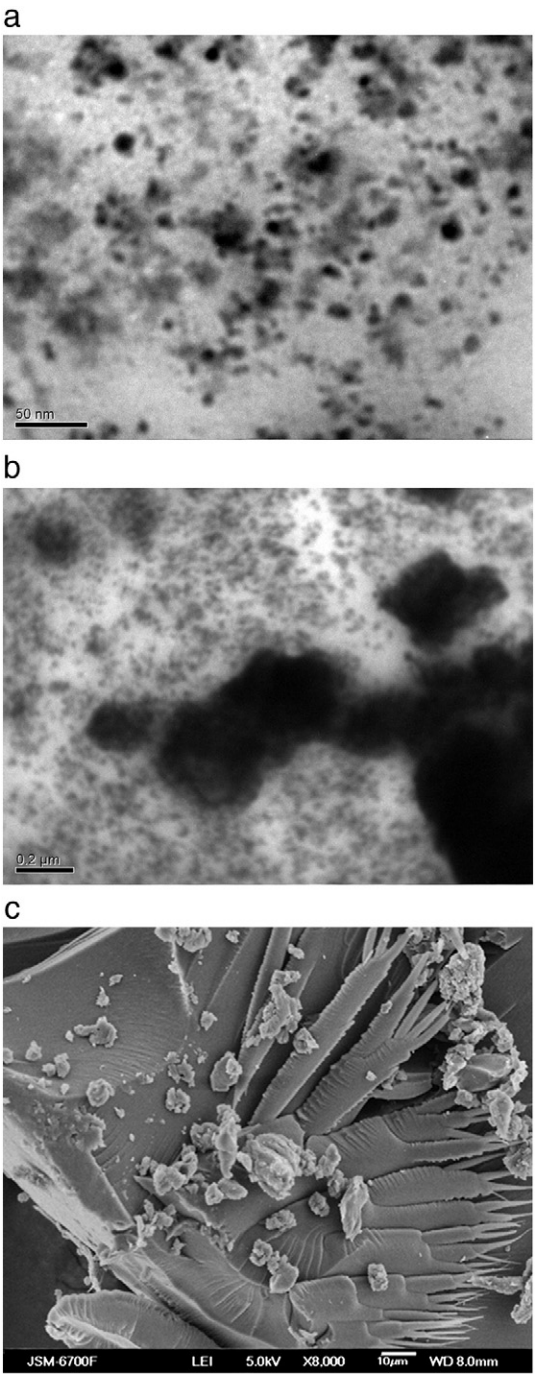

Fig. 1. TEM (a, b) and SEM (c) images of organic–inorganic ion-exchanger.

of the particles in clusters means increase of amount of functional groups there, thus electrostatic repulsion between them becomes stronger. These factors lead to higher swelling of the once modified ion-exchanger comparing with unmodified one. Deterioration of swelling for the samples, which were modified two and more times, can be caused by a decrease of content of osmotically active species in the exchangers [45] due to replacement of strongly acidic $-SO_3H$ groups to weakly acidic ones.

The lowest total ion-exchange capacity ($\overline{A}_{Na,t}$) per volume unit was found for the once modified ion-exchanger evidently due to the highest swelling. Regarding other samples, the $\overline{A}_{Na,t}$ value increases with a decrease of swelling.

The values of ion-exchange capacity ($\overline{A}_{Na}$) vs. solution pH are plotted in Fig. 2. Regarding the unmodified sample, the $\overline{A}_{Na}$ — pH curve is typical

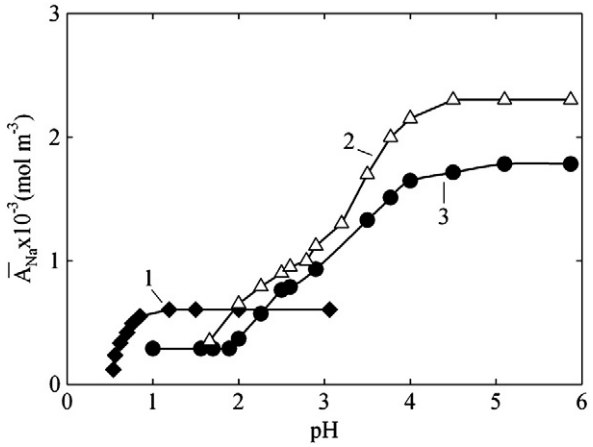

Fig. 2. Ion-exchange capacity of unmodified resin (1), individual ZHP (2) and ion-exchanger modified 8 times (3).

for strongly acidic resins: the plot demonstrates a rapid build-up about pH 1 and then remains without changes. In the case of inorganic material, the curve is seen to be characteristic for weakly acidic ion-exchangers. The steps of the curve correspond to dissociation of dihydrophosphate ($-OPO_3H_2$) groups:

$$-OPO_3H_2 \leftrightarrow -OPO_3H^- + H^+, \quad (2)$$

$$-OPO_3H \leftrightarrow -OPO_3^{2-} + H^+. \quad (3)$$

The second step is also caused by dissociation of hydrophosphate $(-O)_2PO_2H$ groups:

$$(-O)_2PO_2H \leftrightarrow (-O)_2PO_2^- + H^+, \quad (4)$$

Typical $\overline{A}_{Na}$ — pH plot for the composite ion-exchanger contains 3 steps. The first one, which is located in strongly acidic field, is attributed to the polymer, two other steps are related to ZHP.

Electrical conductivity of the ion-exchangers, which was measured at pH 7, demonstrates sufficient growth with ZHP content (see Table 1). This can be explained by increase of mobility of free charge carriers (H^+) and increment of their concentration per volume unit. Analysis of influence of both these factors on conductivity is outside the framework of this paper.

Composite ion-exchangers show higher conductivity than both unmodified resin and individual ZHP.

3.2. Ni^{2+} removal from a solution under dynamic conditions

The dependences of Ni^{2+} concentration at the column outlet (C'_{Ni}) ion-exchanger (V) are plotted in Fig. 3. The field of the curves, which corresponds to minimal nickel content in the solution, becomes wider in the order: individual ZHP, unmodified resin, the samples modified 1-, 4- and 8-times. The unmodified resin sorbs preferably hardness ions (Table 2). The highest removal degree for all the ions as well as the highest ratio of $\frac{C'_{Ca}+C'_{Mg}}{C'_{Ni}}$ have been found for individual ZHP. However the inorganic ion-exchanger is characterized by the lowest break-through capacity towards Ni^{2+} evidently due to low mobility of sorbed ions in ion-exchangers of this type [20,37].

The break-through capacity, $\frac{C'_{Ca}+C'_{Mg}}{C'_{Ni}}$ ratio and Ni^{2+} removal degree tend to rise with an increase of ZHP amount in the polymer. In owing to this, eight modified ion-exchanger, which demonstrates also the highest electrical conductivity, has been chosen for EDI processes.

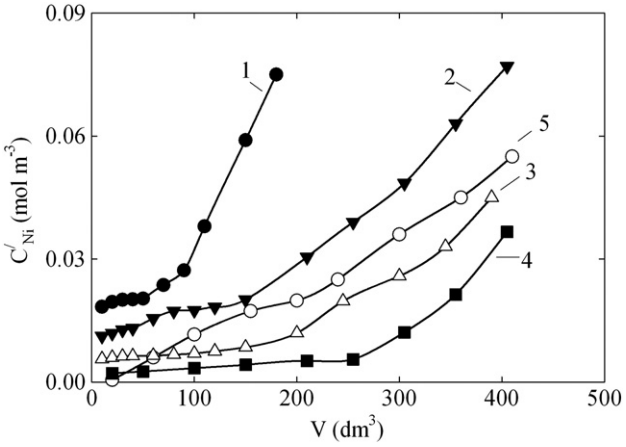

Fig. 3. Ni^{2+} concentration at the column outlet. The solution, which contained (mol m^{-3}): Ni^{2+} — 0.3, Ca^{2+} — 0.9, Mg^{2+} — 0.3, was purified. Unmodified resin (1), resin modified 1 (2), 4 (3), 8 (4) times and ZHP (5) were used.

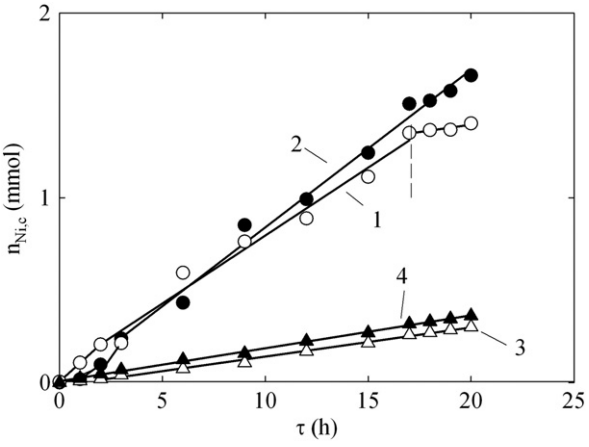

Fig. 4. Ni^{2+} amount in the catholyte as a function of time. Unmodified resin (1), organic–inorganic ion-exchanger (2), ZHP (3), glass particles (4) were used. Dashed line points fouling of unmodified resin. Initial pH of the solution being purified was 3, $v = 3.6$ dm^3 h^{-1}, $C_{Ni} = 0.3$ mol m^{-3}.

3.3. Effect of initial pH of the solution on continuous Ni^{2+} removal

The pH of the initial solution, which contained Ni^{2+}, Ca^{2+}, Mg^{2+} and TOC, was varied in the first series of EDI processes. Typical dependences of Ni^{2+} amount in the catholyte ($n_{Ni,c}$) on time (τ) are shown in Fig. 4. As seen, the plots can be approximated with linear functions within the intervals of 0–20 (glass particles), 1–20 (ZHP, modified resin), 2–17 h (unmodified resin). Deviation from linearity at the initial period for ZHP and organic–inorganic ion-exchanger is due to ion accumulation in solids. Regarding the unmodified resin, rapid ascent ($\tau < 2$ h) is a result of its partial regeneration, since the ion-exchanger was loaded previously with Ni^{2+} ions. The decrease of ion transport rate after 17 h is due to accumulation of organic species by the polymer ion-exchanger. The current also decreased indicating growth of the ion-exchanger resistance. In the case of inert glass particles, the $n_{Ni,c} - \tau$ plot is linear, thus the ion transport is realized through the solution. The slopes of the plots for glass and ZHP are similar, thus the rates of ion transport to the catholyte are equal. This means inertness of the inorganic ion-exchanger after loading with Ni^{2+} ions, no transport through the solid is realized.

After the EDI process was finished, 2.4 mass % additional TOC was for dried unmodified resin, since this material tends to accumulate organic substances. At the same time, no sorption of organics was found for the organic–inorganic ion-exchanger.

Since the rate of ion transport through the cation-exchange membrane was constant during certain period, the results can be represented in a term of ion flux ($N_{Ni,c}$):

$$N_{Ni,c} = \frac{1}{S}\frac{dn_{Ni,c}}{d\tau}, \quad (5)$$

where S is the effective area of the membrane. The flux involves ion transport both through the solution and ion-exchanger. In the cases of glass and ZHP particles, the fluxes are close to each other indicating ion transport through the solution (Fig. 5). The Ni^{2+} removal degree and current efficiency were extremely low, the ratio of $\frac{C'_{Ca}+C'_{Mg}}{C'_{Ni}}$ (where C'_{Ni} is the concentration at the center compartment outlet) was practically similar to that for the initial solution (Table 3).

If the initial solution were neutral, then the lowest fluxes would be found. This is evidently caused by deposition of insoluble nickel compounds in the center compartment. At pH 3, the Ni^{2+} flux is higher for the organic–inorganic resin than for unmodified one, since functional groups of the inorganic constituent are dissociated (see Fig. 2). Thus the composite ion-exchanger is able to uptake preferably Ni^{2+} ions, which are transported to the cathode compartment through the solid. As a result, the ratio of $\frac{C'_{Ca}+C'_{Mg}}{C'_{Ni}}$ is the highest for this ion-exchanger.

Further acidification of the solution causes a decrease of dissociation degree of functional groups of ZHP. This leads to deterioration of Ni^{2+} uptake as well as ion transport to the catholyte. The Ni^{2+} flux is lower than that for the unmodified resin.

Table 2
Removal of Ni^{2+} ions from multicomponent solution under dynamic conditions.[a]

Number of modification cycle	RD_{Ca} (%)	RD_{Mg} (%)	RD_{Ni} (%)	Break-through capacity towards Ni^{2+} (mol m^{-3})	$\frac{C'_{Ca}+C'_{Mg}}{C'_{Ni}}$
0	99.3	99.4	92.8	2.7	0.6
1	98.1	96.1	93.3	8.1	2.2
4	97.4	95.3	95.9	11.4	2.4
8	96.3	91.5	99.8	15.8	15
ZHP	98.4	99.6	99.9	1.3	46

[a] The data are related to break-through capacity towards Ni^{2+}.

3.4. Effect of flow velocity of the solution on continuous nickel removal

Fig. 6 illustrates the effect of flow velocity of the solution (v) on the Ni^{2+} flux to the catholyte. The concentration of species in the solid ($\overline{C}_{Ni}$), at which the $N_{Ni,c}$ value is constant, has been also found from mass balance calculation and confirmed with analysis of the ion-exchanger. Increase of flow velocity (in other words, increment of Ni^{2+} amount in the solution passed through the ion-exchanger bed) causes a rise of

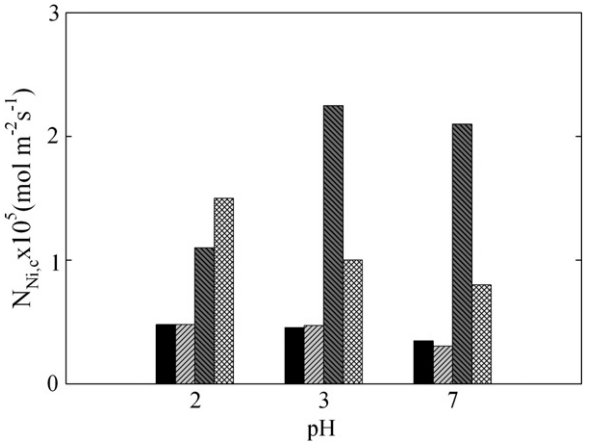

Fig. 5. Ni^{2+} flux to catholyte at different initial pH of the multicomponent solution being purified. Glass particles (■), ZHP (▨), organic–inorganic ion-exchanger (▩) and unmodified resin (▩) were used. Other conditions are pointed in the caption of Fig. 4.

Table 3
Electrodeionization at different pH of the initial solution.

Samples	Ni^{2+} removal degree, %			$\frac{C'_{Ca}+C'_{Mg}}{C_{Ni}}$			Current efficiency (Ni^{2+}), %		
	pH 2	pH 3	pH 7	pH 2	pH 3	pH 7	pH 2	pH 3	pH 7
Unmodified resin	5.0	3.3	2.7	4	4	4.1	5	5	6
Modified resin	3.7	7.5	7.0	4.1	5	5.3	4	10	15
ZHP	1.6	1.5	1.1	4	4	4.1	1	1	2
Glass	1.4	1.5	1.1	4	4	4	1	1	1

the $\overline{C}_{Ni}$ magnitude. The flux through the ion-exchanger ($\overline{N}_{Ni}$) is described by Nernst–Plank equation [45]:

$$\overline{N}_{Ni} = -\left(\overline{D}_{Ni} grad\overline{C}_{Ni} + \frac{z_{Ni}F}{RT}\overline{C}_{Ni}\overline{D}_{Ni} grad\overline{E}\right) + \overline{v}\overline{C}_{Ni} \quad (6)$$

where $\overline{D}_{Ni}$ is the diffusion coefficient of species in the ion-exchanger, z_{Ni} is the charge number, F is the Faraday constant, R is the gas constant, T is the temperature, $grad\overline{E}$ is the potential gradient, which is determined similarly to [40], $\overline{v}$ is the rate of movement of pore liquid. It is assumed, that the pairs of sorbed ions–functional groups are dissociated completely, thus, all sorbed ions are free charge carriers. According to Fig. 5, the flux through the membrane is caused mainly by transport through the ion-exchanger at pH 3, thus $\overline{N}_{Ni} \approx N_{Ni,c}$.

As seen from Fig. 6, the $N_{Ni,c}$–v curve demonstrates a maximum, which is evidently a result of competitions of two factors: increase of Ni^{2+} content in the ion exchanger (improvement of ion transport through the solid) and decrease of $\overline{D}_{Ni}$ value (deterioration of ion transport). As shown earlier for inorganic ion-exchanger [27] and ion-exchange resin [46], the diffusion coefficient of sorbed ions, which is determined from the migration term of Eq. (6), decreases with a growth of their amount in ion-exchanger. Probably this decrease is due to the formation of associated ion pairs of sorbed ions with functional groups of the ion-exchanger, for instance, $(-SO_3^-)_2Ni^{2+} \rightarrow (-SO_3)_2Ni$ similarly to [45]. The concentration of associated pairs in the ion-exchanger evidently increases with growth of content of sorbed ions. Thus, the concentration of free charge carriers ($\overline{C}_{Ni}$), which is used for calculations, is overvalued. As a result, the $\overline{D}_{Ni}$ values are understated. However it is difficult to recognize dissociated and associated pairs. In owing to this, deterioration of ion transport under an increase of content of sorbed ions is usually considered as a result of a decrease of the diffusion coefficient.

The diffusion coefficient can be approximately estimated from the migration term of Eq. (6) using the data of Fig. 6. The contribution of convection term to total conductivity of a flexible resin is up to 6%, if the content of species in the ion-exchanger is rather low [47]. The $\overline{D}_{Ni}$ values were found to reach 3.4×10^{-11} m^2 s^{-1} ($\overline{C}_{Ni} = 28$ mol m^{-3}) and 1.1×10^{-11} m^2 s^{-1} ($\overline{C}_{Ni} = 250$ mol m^{-3}). Increase of Ni^{2+} amount in the ion-exchanger causes deterioration of solution purification (Fig. 7).

If the purification is caused only by sorption followed by ion transport to the catholyte, the formula (1) can be written as:

$$RD = \frac{\Delta n_{Ni,c}}{\Delta n_{Ni,p}} \times 100\%, \quad (7)$$

where $\Delta n_{Ni,p}$ is the amount of species in the solution passed through the ion-exchanger during certain time. Formula (7) is valid, when the flux of ions to the concentration compartment is constant. The removal degree is 100% at $\Delta n_{Ni,c} = \Delta n_{Ni,p}$. This equality can be expressed as $\frac{dn_{Ni,c}}{d\tau} = \frac{dn_{Ni,p}}{d\tau}$ in the case of $\Delta\tau \rightarrow 0$. Thus $\frac{dn_{Ni,p}}{d\tau} - \frac{dn_{Ni,c}}{d\tau} = 0$ for $RD = 100\%$. Extrapolation of the curve of $\frac{dn_{Ni,p}}{d\tau} - \frac{dn_{Ni,c}}{d\tau}$ vs. v to X-axis gives the rate, at which Ni^{2+} species can be removed completely ($v = 0.3$ dm^3 h^{-1} or linear velocity of 8.3×10^{-4} m s^{-1}, $C_{Ni} = 0.3$ mol m^{-3} and $U = 5$ V).

3.5. Effect of initial concentration of the solution on continuous Ni^{2+} removal

The initial concentration of Ni^{2+} ions in the solution was varied in other series of experiments. The N_{Ni}–C_{Ni} plot demonstrates rapid ($C_{Ni} = 0.3$–2 mol m^{-3}) and slow ($C_{Ni} > 2$ mol m^{-3}) growth with increase of Ni^{2+} content in the initial solution (Fig. 8). The slow increase of Ni^{2+} flux at $C_{Ni} > 2$ mol m^{-3} is evidently caused by deposition of insoluble Ni^{2+} compounds inside the center compartment. This is confirmed by a gradual decrease of current in time on the one hand and analysis of mass balance on the other hand.

It is also possible to estimate, whether the solution purification is caused only by sorption followed by ion transport to the catholyte. The formula (7) can be also written as:

$$RD = \frac{dn_{Ni,c}}{d\tau}\left(\frac{dn_{Ni,p}}{d\tau}\right)^{-1} \times 100\%. \quad (8)$$

At the same time the expression (1) gives the purification degree caused also by deposition inside the center compartment. As seen from Fig. 8, the RD values calculated according to formula (1) are higher than those obtained using expression (8) at $C_{Ni} > 1.2$ mol m^{-3}. Thus Ni^{2+} removal is a result of electrodeionization and deposition inside center compartment under these conditions. Moreover, insoluble deposit is visible on the ion-exchanger particles after the end of the

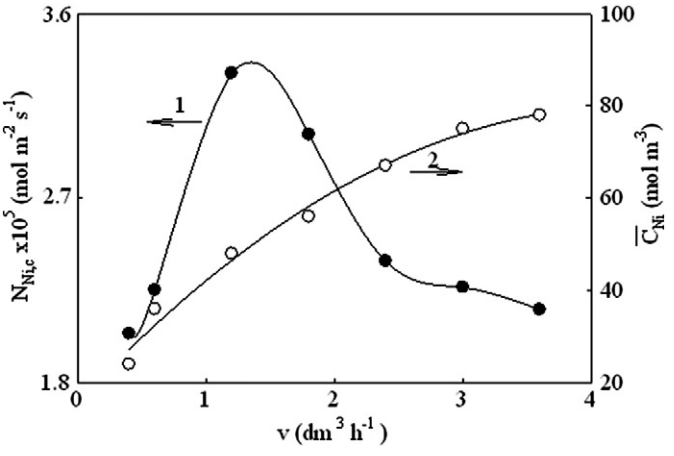

Fig. 6. Ni^{2+} flux to the catholyte (1) and Ni^{2+} concentration in the ion exchanger (2) under equality of rates of ion exchange and transport to the catholyte as functions of flow velocity of the solution, $C_{Ni} = 0.3$ mol m^{-3}. The initial pH of the solution was 3. Organic–inorganic ion-exchanger was used.

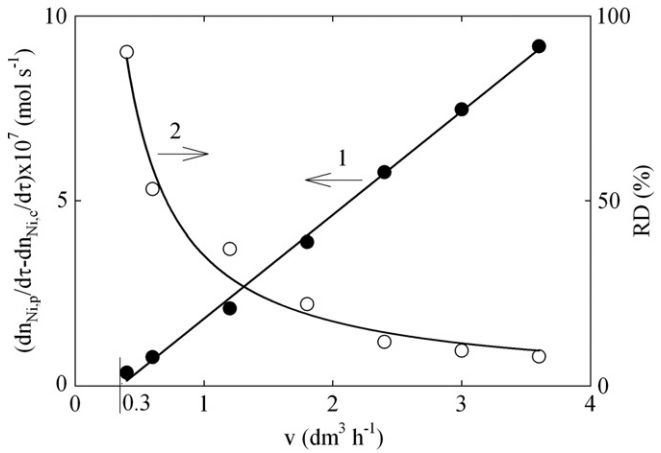

Fig. 7. $\frac{dn_{Ni,p}}{d\tau} - \frac{dn_{Ni,c}}{d\tau}$ difference (1) and Ni^{2+} removal degree (2) as functions of flow velocity of the solution through the center compartment. Other experimental conditions are pointed in the caption of Fig. 6.

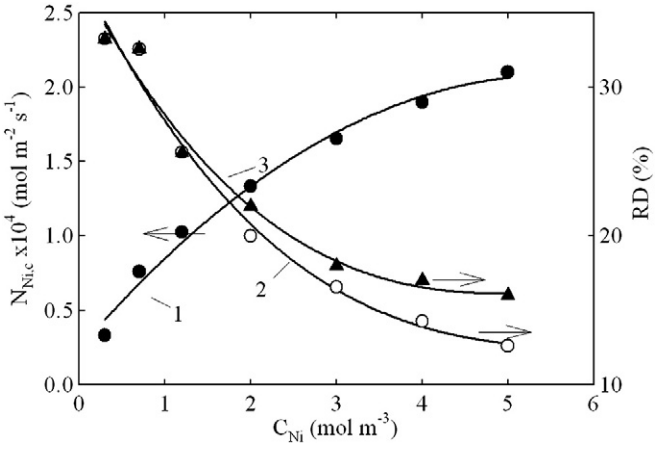

Fig. 8. Flux of Ni^{2+} ions to the catholyte (1) and their removal degree (2, 3) as functions of initial concentration of the solution. The values of removal degree were calculated according to: 2 — formula (8), 3 — formula (1). The initial pH of the solution was 3, $\nu = 1.2$ dm^3 h^{-1}.

experiment. The deposition is caused by water split at the interface between particles and solution [15]. H^+ ions replace counter-ions of fixed groups of the ion-exchanger, which move towards the cation-exchange membrane. This replacement causes increase of OH^- ion concentration in the solution at the particle surface. If the concentration of the initial solution is low, the experimental and calculated *RD* values are practically equal indicating an absence of deposition. Moreover, a decrease of initial Ni^{2+} content in the solution leads to an increase of $\frac{C'_{Ca}+C'_{Mg}}{C'_{Ni}}$ ratio due to preferable Ni^{2+} sorption (Fig. 9).

Extrapolation of the plot of $\frac{dn_{Ni,p}}{d\tau} - \frac{dn_{Ni,c}}{d\tau}$ vs. C_{Ni} gives the initial Ni^2 concentration, at which these species can be removed completely. This concentration is estimated as 0.15 mol m^{-3}. Another condition, at which the complete purification degree can be reached, are: $\nu = 1.2$ dm^3 h^{-1}, $U = 5$ V and initial pH of the solution about 3.

3.6. Long-time electrodeionization

The first long-time EDI process was carried out based on results of the experiments, in which the flow velocity through the ion-exchanger bed was varied. As found, the $\frac{dn_{Ni,p}}{d\tau} - \frac{dn_{Ni,c}}{d\tau}$ difference is close to 0 at $\nu = 0.3$ dm^3 h^{-1} and initial Ni^{2+} concentration of 0.3 mol m^{-3} (see Fig. 7). Thus, complete Ni^{2+} removal should be expected under these conditions. The mentioned flow velocity is related to the cell 1, the linear velocity (ω) corresponds to 8.3×10^{-4} m s^{-1} in this case. Regarding the cell 2, the flow velocity should be 3 dm^3 h^{-1}. Indeed residual Ni^{2+} concentration in the solution at the outlet of the center compartment is lower than 1 ppm during the long-time EDI process (Table 4). As seen from Fig. 10, the ratio of fluxes of species to their initial concentration in the solution is the highest for Ni^{2+} ions. This indicates preferable Ni^{2+} removal from the low-concentrated solution. During the process, the Ni^{2+}-containing solution was acidified directly in the center compartment due to ion exchange on the one hand and leakage of acid through an anion-exchange membrane (similarly to [40]) on the other hand.

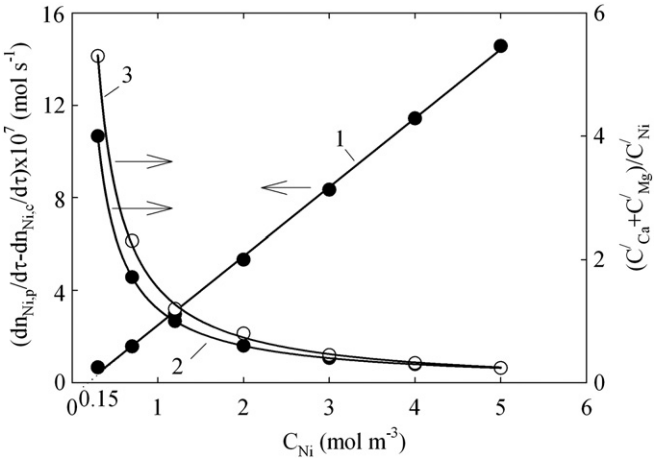

Fig. 9. $\frac{dn_{Ni,p}}{d\tau} - \frac{dn_{Ni,c}}{d\tau}$ difference (1), $\frac{C'_{Ca}+C'_{Mg}}{C'_{Ni}}$ ratios in inlet (2) and outlet (3) of the center compartment as functions of initial concentration of the solution. Other conditions are pointed in the caption of Fig. 8.

However the removal degree is lower than 100%. This is probably caused by a competition between sorption and desorption at pH 2.5, since the inorganic constituent of the composite ion-exchanger contains weakly acidic groups.

Let us make some quantitative assessments to estimate the Ni^{2+} flux through the solution. The mass transport coefficient (k_{Ni}) can be found from the equation, which has been developed for three-dimensional electrode [48]:

$$\frac{k_{Ni}\bar{d}}{D_{Ni}} = 1.52\left(\frac{\omega\bar{d}}{\upsilon}\right)^{0.55}\left(\frac{\upsilon}{D_{Ni}}\right)^{0.33} \quad (9)$$

where υ is the viscosity, $\bar{d}$ is the particle diameter. Since $\upsilon = 9 \times 10^{-7}$ m^{2}s^{-1}, $D_{Ni} = 6.5 \times 10^{-10}$ m^{2}s^{-1} [49], $\bar{d} = 4 \times 10^{-4}$ m (as found with SEM), the k_{Ni} value was estimated as 1.5×10^{-5} m s^{-1}. Under conditions of limiting current, the diffusion flux of Ni^{2+} ions is determined as $k_{Ni}C_{Ni}$ (sufficient excess of other cations) or $k_{Ni}C_{Ni}\left(1 + \frac{z_{Ni}}{|z_{An}|}\right)$ (concentrations of Ni^{2+} and other cations are comparable) [50]. The flux is 4.6×10^{-6}–9×10^{-6} mol m^{-2} s^{-1} due to diffusion through a hydrodynamically immobile solution layer at the membrane surface. The migration flux of Ni^{2+} species through bulk of a solution can be determined as $\frac{it_{Ni}}{z_{Ni}F}$ [49], where i is the current density, t_{Ni} is the transport number of species through a solution. The transport number is determined as $\frac{z_{Ni}^2F^2C_{Ni}D_{Ni}}{RT\kappa}$ [48], where κ is the electrical conductivity of the solution. Since $\kappa = 0.13\ \Omega^{-1}$ m^{-1}, $i = 40$ A m^{-2}, the transport number of Ni^{2+} species were estimated as 2.2×10^{-2}. Thus, the migration flux is 4.6×10^{-6} mol m^{-2} s^{-1}. The experimental flux (2.5×10^{-5} mol m^{-2} s^{-1}) is much higher compared with the calculated values indicating transport of species mainly from the ion-exchanger bed. The energy consumption, which were determined as $iSU\tau$ (where τ is the time, which is necessary for purification of 1 m^3 solution), is 0.7 kWh (without equipment).

The second experiment was performed using the data of Fig. 9. The concentration, at which the highest removal degree is expected, was found as 0.15 mol m^{-3} at flow velocity of 1.2 dm^3 h^{-1} (this corresponds to $\omega = 3.3 \times 10^{-3}$ m s^{-1} or 12 dm^3 h^{-1} for cell 2). The highest rate of ion transport is reached at this flow velocity (see Fig. 6). As seen from Fig. 10, Ni^{2+} species are removed preferably

Table 4
Ni^{2+} removal during long-time EDI process at 5 V.

ν, dm^{-3} h^{-1}	C_{Ni}, mol m^{-3}	i, A m^{-3}	Solution at the outlet of center compartment					Current efficiency (Ni^{2+}), %
			pH	κ, Ohm^{-1} m^{-1}	Residual concentration, ppm			
					Ni^{2+}	Ca^{2+}	Mg^{2+}	
3	0.30	40	2.5	0.13	0.7	3.1	2.1	12
12	0.15	95	2.3	0.20	0.9	3.2	1.1	10

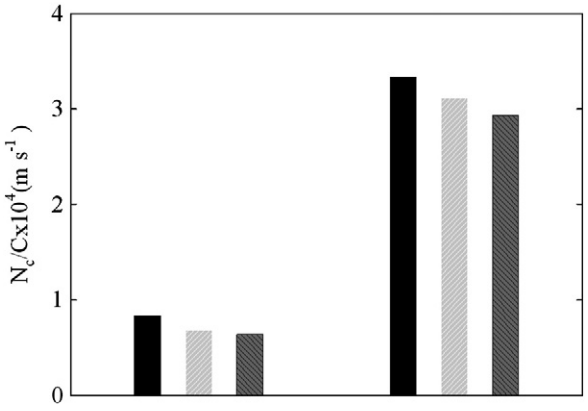

Fig. 10. $\frac{N}{C}$ ratio for Ni^{2+} (■), Ca^{2+} (▨), Mg^{2+} (▩) during long-time electrodeionization of Ni^{2+}-containing solution. $1-\nu = 3$ dm^3 h^{-1}, $C_{Ni} = 0.3$ mol m^{-3}; $2-\nu = 12$ dm^3 h^{-1}, $C_{Ni} = 0.15$ mol m^{-3}.

under these conditions. The energy consumptions of the process are 0.4 kWh.

4. Conclusions

Organic–inorganic ion-exchangers have been obtained by modification of gel-like flexible resin with ZHP nanoparticles, which exist in the polymer both in non-aggregated and aggregated forms. The increase of content of the inorganic constituent up to 40.1 mass % causes an improvement of Ni^{2+} removal from the solution, which contains also Ca^{2+}, Mg^{2+} and TOC, under dynamic open circuit conditions. Moreover, organic–inorganic ion-exchangers demonstrate higher electric conductivity in comparison with both unmodified resin and individual ZHP. The resin containing 40.1% ZHP has been chosen for EDI process, since the highest total ion-exchange capacity (towards Na^+), break-through capacity (towards Ni^{2+}), and electrical conductivity were found for this ion-exchanger. Unfortunately, further increase of inorganic constituent leads to deterioration of mechanical stability of particles.

The diffusion coefficients of Ni^{2+} ions through the organic–inorganic ion-exchanger has been estimated as 1.1×10^{-11}–3.4×10^{-11} m^2 s^{-1}, this is of the same order of magnitude as the $\overline{D}$ value for unmodified flexible ion-exchange resin [20,51].

Regarding the EDI process, the organic–inorganic ion-exchanger demonstrates higher Ni^{2+} flux to the catholyte and higher removal degree in comparison with unmodified resin. This is valid for the field of initial pH of the solution, at which functional groups of ZHP are dissociated. However, deposition of insoluble nickel compounds in the center compartment deteriorates Ni^{2+} recovery from neutral solution. The organic–inorganic ion-exchanger was found to demonstrate stability against fouling with organic substances in opposite to unmodified resin. The processes of Ni^{2+} removal from low-concentrated multicomponent solutions (0.15–0.30 mol m^{-3} Ni^{2+}) were developed based on the study of ion transport under variation of initial concentration and flow velocity of the solution. Residual Ni^{2+} content in the purified solution is 0.7–0.9 ppm; the energy consumptions are 0.4–0.7 kWh per 1 m^3. The processes are realized according to "once-through operation" in opposite to [19], they allow us to remove Ni^{2+} from solutions, which contain also Ca^{2+}, Mg^{2+} and TOC. Thus the organic–inorganic ion-exchanger is more attractive than unmodified flexible resin, which removes preferably hardness ions [19,20]. The composite material is chemically and mechanically stable in opposite to ZHP hydrogel, which was used earlier for EDI process [27].

Improvement of the process productivity requires further development of cell configuration. First of all, the development should provide increase of ion-exchanger volume. Correction of the purified solution pH has to be also provided simultaneously with Ni^{2+} removal. This is a subject of further investigations.

List of symbols

$\overline{A}$	total ion-exchange capacity (mol m^{-3});
$\overline{C}$	initial concentration of species in solution (mol m^{-3});
C'	concentration of species in solution after purification (mol m^{-3});
$\overline{C}$	concentration of species in ion-exchanger (mol m^{-3});
D	diffusion coefficient of species in solution (m^{2}s^{-1});
$\overline{D}$	diffusion coefficient of species in ion-exchanger (m^{2}s^{-1});
$\overline{d}$	particle diameter (m);
$\overline{E}$	potential drop across ion-exchange bed (V);
F	Faraday constant (A s mol^{-1});
i	current density (A);
k	mass transport coefficient (m s^{-1});
N	flux of species through the membrane (mol m^{-1} s^{-1});
$\overline{N}$	flux of species through ion-exchanger (mol m^{-1} s^{-1});
n_c	amount of species in the catholyte (mol);
n_p	amount of species in the solution passed through the ion-exchanger bed (mol);
R	universal gas constant (J mol^{-1} K^{-1});
RD	removal degree, %;
S	surface (m^2);
T	temperature (K);
t	transport number;
U	cell voltage (V)
V	volume of solution (dm^3);
v	velocity of solution (dm^3 h^{-1}):
z	charge number.

Greeks

κ	conductivity of a solution (Ohm^{-1} m^{-1});
υ	viscosity (m^{2}s^{-1});
$\overline{v}$	rate at which the center of gravity of the pore liquid moves (m s^{-1});
τ	time (s or h);
ω	linear flow velocity (m s^{-1}).

Abbreviations

An	anions;
DVB	divinylbenzene
EDI	electrodeionization$
TOC	total organic carbon;
ZHP	zirconium hydrophosphate.

Acknowledgments

The work was supported by projects within the framework of programs supported by the Government of Ukraine "Nanotechnologies and nanomaterials" (grant No. 6.22.1.7), and the NAS of Ukraine "Problems of stabile development, rational nature management and environmental saving" (grant No. 30-11), and "Materials for ion exchange and baromembrane processes of water desalination" (grant No. 93/2-221).

References

[1] E. Glueckauf, Electro-deionisation through a packed bed, Br. Chem. Eng. 4 (1959) 646–651.
[2] Ö. Arar, Ü. Yüksel, N. Kabay, M. Yüksel, Demineralization of geothermal water reverse osmosis (RO) permeate by electrodeionization (EDI) with layered bed configuration, Desalination 317 (2013) 48–54.
[3] Ö. Arar, Ü. Yüksel, N. Kabay, M. Yüksel, Application of electrodeionization (EDI) for removal of boron and silica from reverse osmosis (RO) permeate of geothermal water, Desalination 310 (2013) 25–33.
[4] J. Bi, C. Peng, H. Xu, A.-S. Ahmed, Removal of nitrate from groundwater using the technology of electrodialysis and electrodeionization, Desalin. Water Treat. 34 (2011) 394–401.

[5] J.-S. Park, J.-H. Song, K.-H. Yeon, S.-H. Moon, Removal of hardness ions from tap water using electromembrane processes, Desalination 202 (2007) 1–8.
[6] N. Meyer, W.J. Parker, P.J. Van Geel, M. Adiga, Development of an electrodeionization process for removal of nitrate from drinking water Part 1: single-species testing, Desalination 175 (2005) 153–165.
[7] N. Meyer, W.J. Parker, P.J. Van Geel, M. Adiga, Development of an electrodeionization process for removal of nitrate from drinking water. Part 2: multi-species testing, Desalination 175 (2005) 167–177.
[8] C. Larchet, V.I. Zabolotsky, N.D. Pismenskaya, V.V. Nikonenko, A. Tskhay, K. Tastanov, G. Pourcelly, Comparison of different ED stack conceptions when applied for drinking water production from brackish waters, Desalination 222 (2008) 489–496.
[9] J. Wood, Continuous electrodeionization for water treatment at power plants, Power Eng. 112 (2008) 62–66.
[10] A. Dey, B. Loyd, N. Roades, A case study in the use of EDI for boiler make-up water, Ultrapure Water 24 (2007) 17–24.
[11] D. Mittal, V.J. Nathan, Use of unique fractional electrodeionization in power plant applications, Ultrapure Water 27 (2010) 24–32.
[12] M.B.C. Elleuch, M.B. Amor, G. Pourcelly, Phosphoric acid purification by a membrane process: electrodeionization on ion-exchange textiles, Sep. Purif. Technol. 51 (2006) 285–290.
[13] P. Yu, Z. Zhu, Y. Luo, Y. Hu, S. Lu, Purification of caprolactam by means of an electrodeionization technique, Desalination 174 (2005) 231–235.
[14] N. Harada, T. Otomo, T. Watabe, T. Ase, T. Takemura, T. Sato, Removal of viable bacteria and endotoxins by Electro Deionization (EDI), Biocontrol Sci. 16 (2011) 109–115.
[15] V.D. Grebenyuk, V.M. Linkov, N.A. Linkov, J.J. Smit, Electroadsorption of Ni^{2+} ions in an electrodialysis chamber containing granulated ion-exchange resin, J. Appl. Electrochem. 28 (1998) 1189–1193.
[16] P.B. Spoor, L. Koene, W.R. ter Veen, L.J.J. Janssen, Electrodeionization 3: the removal of nickel from dilute solutions, J. Appl. Electrochem. 32 (2002) 1–10.
[17] P.B. Spoor, L. Koene, L.J.J. Janssen, Electric potential and concentration gradient in a hybrid ion-exchange electrodialysis system, J. Appl. Electrochem. 32 (2002) 369–377.
[18] P.B. Spoor, L. Koene, W.R. ter Veen, L.J.J. Janssen, Continuous deionization of a dilute nickel solution, Chem. Eng. J. 85 (2001) 127–135.
[19] P.B. Spoor, L. Grabovska, L. Koene, L.J.J. Janssen, W.R. ter Veen, Pilot scale deionization of a galvanic nickel solution using a hybrid ion-exchange/electrodialysis system, Chem. Eng. J. 89 (2002) 193–202.
[20] Yu.S. Dzyazko, L.M. Rozhdestvenska, A.V. Palchik, Recovery of nickel ions from dilute solutions by electrodialysis combined with ion exchange, Russ. J. Appl. Chem. 78 (2005) 414–421.
[21] A. Mahmoud, L. Muhr, G. Grévillot, F. Lapicque, Experimental tests and modelling of an electrodeionization cell for the treatment of dilute copper solutions, Can. J. Chem. Eng. 85 (2007) 171–179.
[22] A. Mahmoud, A.F.A. Hoadley, An evaluation of a hybrid ion exchange electrodialysis process in the recovery of heavy metals from simulated dilute industrial wastewater, Water Res. 46 (2012) 3364–3376.
[23] H.-J. Lee, M.-K. Hong, S.-H. Moon, A feasibility study on water softening by electrodeionization with the periodic polarity change, Desalination 284 (2012) 221–227.
[24] Ö. Arar, Ü. Yüksel, N. Kabay, M. Yüksel, Removal of Cu2 + ions by a micro-flow electrodeionization (EDI) system, Desalination 277 (2011) 296–300.
[25] H. Dong, J. Wang, H. Lu, H. Yu, Nickel-containing effluent reclaming by bipolar membrane-electrodeionization process, Adv. Mater. Res. 233–235 (2011) 942–948.
[26] Yu.S Dzyaz'ko, L.N. Ponomareva, Y.M. Vol'fkovich, V.E. Sosenkin, V.N. Belyakov, Conducting properties of a gel ionite modified with zirconium hydrophosphate nanoparticles, Russ. J. Electrochem. 49 (2013) 209–215.
[27] L.M. Rozhdestvenska, Yu.S. Dzyazko, V.N. Belyakov, Electrodeionization of a Ni^{2+}-containing solution using highly hydrated zirconium hydrophosphate, Desalination 198 (2006) 247–255.
[28] B. Pan, Q. Zhang, W. Du, W. Zhang, B. Pan, Q. Zhang, Z. Xu, Q. Zhang, Selective heavy metals removal from waters by amorphous zirconium phosphate: behavior and mechanism, Water Res. 41 (2007) 3103–3111.
[29] S. Yu, V.V. Dzyaz'ko, L.M. Trachevskii, S.L. Rozhdestvenskaya, V.N. Belyakov Vasilyuk, Interaction of sorbed Ni(II) ions with amorphous zirconium hydrogen phosphate, Russ. J. Phys. Chem. A 87 (2013) 840–845.
[30] B.C. Pan, Q.R. Zhang, W.M. Zhang, B.J. Pan, W. Du, L. Lv, Q.J. Zhang, Z.W. Xu, Q.X. Zhang, Highly effective removal of heavy metals by polymer-based zirconium phosphate: a case study of lead ion, J. Colloid Interface Sci. 310 (2007) 99–105.
[31] Q.R. Zhang, W. Du, B.C. Pan, B.J. Pan, W.M. Zhang, Q.J. Zhang, Z.W. Xu, Q.X. Zhang, A comparative study on Pb^{2+}, Zn^{2+} and Cd^{2+} sorption onto zirconium phosphate supported by a cation exchanger, J. Hazard. Mater. 152 (2008) 469–475.
[32] B. Pan, B. Pan, X. Chen, W. Zhang, X. Zhang, Q. Zhang, Q. Zhang, J. Chen, Preparation and preliminary assessment of polymer-supported zirconium phosphate for selective lead removal from contaminated water, Water Res. 40 (2006) 2938–2946.
[33] Q. Zhang, B. Pan, S. Zhang, J. Wang, W. Zhang, L. Lv, New insights into nanocomposite adsorbents for water treatment: a case study of polystyrene-supported zirconium phosphate nanoparticles for lead removal, J. Nanoparticle Res. 13 (2011) 5355–5364.
[34] Yu.S. Dzyazko, L.N. Ponomaryova, Yu.M. Volfkovich, V.E. Sosenkin, V.N. Belyakov, Polymer ion-exchangers modified with zirconium hydrophosphate for removal of Cd^{2+} ions from diluted solutions, Sep. Sci. Technol. 48 (2013) 2140–2149.
[35] V. Coman, B. Robotin, P. Ilea, Nickel recovery/removal from industrial wastes: a review, Resour. Conserv. Recycl. 73 (2013) 229–238.
[36] Yu.S. Dzyazko, L.N. Ponomareva, Yu.M. Volfkovich, V.E. Sosenkin, Effect of the porous structure of polymer on the kinetics of Ni^{2+} exchange on hybrid inorganic–organic ionites, Russ. J. Phys. Chem. A 86 (2012) 913–919.
[37] Yu. Dzyazko, L. Rozhdestvenska, A. Palchik, F. Lapicque, Ion-exchange properties and mobility of Cu^{2+} ions in zirconium hydrophosphate ion exchangers, Sep. Purif. Technol. 45 (2005) 141–146.
[38] M. Marhol, Ion Exchangers in Analytical Chemistry, Academia, Prague, 1982.
[39] E. Heymann, J. O'Donnell, Physicochemical investigation of a cation exchange resin (amberlite IR100) I. Resin equilibria, J. Colloid Sci. 4 (1949) 395–404.
[40] Yu.S. Dzyazko, V.N. Belyakov, Purification of a diluted nickel solution containing nickel by a process combining ion exchange and electrodialysis, Desalination 162 (2004) 179–189.
[41] Yu.S. Dzyazko, L.M. Rozhdestvenskaya, S.L. Vasilyuk, V.N. Belyakov, N. Kabay, M. Yuksel, Ö. Arar, Ü. Yüksel, Electrodeionization of Cr (VI)-containing solution. Part I: chromium transport through granulated inorganic ion-exchanger, Chem. Eng. Commun. 3 (21) (2009).
[42] S.J. Clark, Quantitative Methods of Organic Microanalysis, Butterworth Scientific Publications, London, 1956.
[43] V.I. Zabolotsky, V.V. Nikonenko, Effect of structural membrane inhomogeneity on transport properties, J. Membr. Sci. 79 (1993) 181–198.
[44] W.Y. Hsu, T.D. Gierke, Ion transport and clustering in nafion perfluorinated membranes, J. Membr. Sci. 13 (1983) 307–326.
[45] F. Helfferich, Ion Exchange, Dover, New York, 1995.
[46] P.B. Spoor, L. Koene, W.R. ter Veen, L.J.J. Janssen, Electrodeionization 1. The migration of nickel ions in a rigid, macroporous cation-exchange resin, J. Appl. Electrochem. 31 (2001) 523–530.
[47] Yu.S. Dzyazko, V.M. Linkov, V.N. Belyakov, Electrical conductivity of a flexible resin loaded with Cr (III) ions, Desalination 241 (2009) 57–67.
[48] F. Walsh, A First Course in Electrochemical Engineering, Alresford Press, London, 1993.
[49] R. Parsons, Handbook of Electrochemical Constants, Butterworth Scientific Publications, London, 1959.
[50] K.J. Vetter, Electrochemishe Kinetik, Springer, Berlin, 1961.
[51] P.B. Spoor, L. Koene, W.R. ter Veen, L.J.J. Janssen, Electrodeionization 2, the migration of nickel ions absorbed in a flexible ion-exchange resin, J. Appl. Electrochem. 31 (2001) 1071–1077.